An Improved Bioluminescence Resonance Energy Transfer Strategy for Imaging Intracellular Events in Single Cells and Living Subjects

Abhijit De, Andreas Markus Loening, and Sanjiv Sam Gambhir

Molecular Imaging Program at Stanford and Bio-X Program, Departments of Radiology and Bioengineering, School of Medicine, Stanford University, Stanford, California

Abstract

Bioluminescence resonance energy transfer (BRET) is currently used for monitoring various intracellular events, including protein-protein interactions, in normal and aberrant signal transduction pathways. However, the BRET vectors currently used lack adequate sensitivity for imaging events of interest from both single living cells and small living subjects. Taking advantage of the critical relationship of BRET efficiency and donor quantum efficiency, we report generation of a novel BRET vector by fusing a GFP^2 acceptor protein with a novel mutant *Renilla* luciferase donor selected for higher quantum yield. This new BRET vector shows an overall 5.5-fold improvement in the BRET ratio, thereby greatly enhancing the dynamic range of the BRET signal. This new BRET strategy provides a unique platform to assay protein functions from both single live cells and cells located deep within small living subjects. The imaging utility of the new BRET vector is shown by constructing a sensor using two mammalian target of rapamycin pathway proteins (FKBP12 and FRB) that dimerize only in the presence of rapamycin. This new BRET vector should facilitate high-throughput sensitive BRET assays, including studies in single live cells and small living subjects. Applications will include anticancer therapy screening in cell culture and in small living animals. [Cancer Res 2007;67(15):7175–83]

Introduction

Interactions of proteins are critical for many biological processes including signal transduction. Signal transduction frequently involves many regulatory proteins that enhance cell proliferation in response to extracellular stimuli and, therefore, aberrant mutations in these regulatory proteins are often potential targets for cancer management (1). An example of one such regulatory network is the mammalian target of rapamycin (mTOR) signaling pathway. Deregulation of this pathway is shown to have a profound effect in diverse human diseases including cancer (2, 3), and small molecules (rapamycin and its analogues) that target mTOR pathway proteins are attractive therapeutic candidates with increasing clinical interest. In the scenario where either the genetic mutations or the antiproliferative agents demand rapid screening procedures, optical reporter–based functional imaging assays would be ideal. Currently, assays to identify and characterize these interactions are primarily *in vitro* binding assays (4–6). In the past 5 years, imaging strategies based on yeast two-hybrid assays, reporter complementation assays, and resonance energy transfer–based assay methods (7–12) have been developed. However, all of these approaches have encountered shortcomings, limiting their potential to serve as a single imaging assay for measuring protein-protein interactions from both single cells and physiologically relevant small living animal models.

In the context of imaging oncogenic cellular events from small animal models, bioluminescence approaches have the potential to be much more sensitive than similar fluorescent or radionuclide-based approaches (13, 14). Several adaptations of bioluminescence imaging have already been devised by our lab and others to detect protein functions and protein interactions in small living animals, such as the inducible luciferase yeast two-hybrid system (15, 16), luciferase complementation (17–21), and, more recently, bioluminescence resonance energy transfer (BRET; refs. 22, 23). Although these approaches show promise in detecting signal from specific protein-protein interactions within small animal subjects, their sensitivity to measure such events from single live cells and from deep tissues within animals is limited. Due to the fact that the emissions from luciferases usually yield very low levels of light, counting sufficient photons to estimate brightness from a small area typically requires long acquisition times, thus limiting existing techniques in achieving single-cell sensitivity. This single-cell sensitivity may be particularly important if one wants to study heterogeneous behavior of individual cells instead of being limited to studying the bulk behavior of groups of cells.

BRET is an emerging, nondestructive, cell-based assay technique that allows detection of protein interactions in real time, thus providing a new window for various proteomics applications including receptor-ligand interactions and mapping of signal transduction pathways, etc. This technique is based on a nonradiative energy transfer between two fusion proteins, with one protein containing a bioluminescent moiety as an energy donor and the other protein a fluorescent moiety serving as the energy acceptor. To date, in most BRET applications, the donor moiety is Renilla luciferase (*Rluc*) and the acceptor moiety is the yellow fluorescent protein (24). A second system, referred to as BRET^2 (25), provides for better spectral resolution by using a mutant of the green fluorescent protein (GFP^2) as the acceptor and switching the native RLUC substrate, coelenterazine, with the analogue coelenterazine-400a (Clz400; also known as DeepBlueC). GFP^2 is an *Aequorea victoria* GFP mutant adapted for excitation at 400 nm while retaining its 515-nm peak emission. Clz400 is similar to the native substrate in being cell-permeable and nontoxic, but it differs by yielding a 400-nm emission peak rather than the 485-nm

Note: Supplementary data for this article are available at Cancer Research Online (http://cancerres.aacrjournals.org/).

Requests for reprints: Sanjiv Sam Gambhir, Bio-X Program, Departments of Radiology and Bioengineering, The James H. Clark Center, Stanford University School of Medicine, 318 Campus Drive, E150, Stanford, CA 94305-5427. Phone: 650-725-2309; Fax: 650-897-9988; E-mail: Sgambhir@stanford.edu.

doi:10.1158/0008-5472.CAN-06-4623

peak of the native substrate. In this study, we describe the development of new BRET vectors by fusing a mutated *Renilla* donor protein with the GFP^2 acceptor to achieve a significantly higher BRET efficiency. The new vector is capable of imaging BRET signal from live single cells as well as from superficial and deep tissue structures of small animal models while using a cooled charge-coupled device (CCD) camera–based spectral imaging technique. Furthermore, by incorporating a sensor within the new BRET vector based on rapamycin-dependent interacting partners from the mTOR pathway, we tested the utility of the system for imaging small-molecule dimerizer drug efficacies from intact living single cells.

Materials and Methods

Materials. *pGFP^2-Rluc*, *phRluc-N*, and *pGFP^2-C* plasmids were from Perkin-Elmer. Clz400 was from the Molecular Imaging Products Company. Zeocin, geneticin, and all cell culture media were from Invitrogen. Superfect transfection reagent was from Qiagen. 10% Tris-HCl ReadyGels were from Bio-Rad. *Renilla* luciferase monoclonal antibody (mAb 4400) was from Chemicon, Living color A.V. peptide antibody was from Clontech, and α-tubulin monoclonal antibody was from Sigma. BRET^2 specific 370 to 450 nm (donor) and 500 to 570 nm (acceptor) filters were from Chroma. Black box CCD imaging systems (IVIS100 or IVIS200) were from Caliper (formerly Xenogen). Three- to four-week-old nude mice (*nu/nu*) were from Charles River Laboratories.

Plasmid construct. pBRET^2 (pCMV-*GFP^2*-MCS-*Rluc*) was used as the template for making BRET vectors. Fusion constructs were made by cloning single-mutation C124A *Rluc*, double-mutation C124A/M185V *Rluc*, or *Rluc8* to replace the *Rluc* donor sequence (these *RLuc* variants are described below). The two mTOR pathway proteins, FKBP12 and single FRAP binding domain (FRB), were PCR amplified and cloned using suitable restriction enzyme sites from the multiple cloning site of the control vector. All products were checked by sequencing. All clonal selections were done on bacto-agar plate with zeocin.

Western blotting. Expression of fusion constructs was verified in mammalian cells using 293T or HT1080 cells. Twenty-four hours posttransfection, cells were harvested and lysed on ice using cell lysis buffer (Cell Signaling). Equal amounts of lysates were run on 10% Tris-HCl ReadyGels and transferred onto nitrocellulose membrane (Amersham) with a semidry blotting system. The blots were probed with either *Renilla* antibody or Living color antibody to detect RLUC or GFP^2, respectively. The α-tubulin antibody was used as loading control.

Cell culture, transfection, clonal isolation, and luciferase assay. Human 293T embryonic kidney cells [American Type Culture Collection (ATCC)] were grown in MEM supplemented with 10% fetal bovine serum (FBS) and 1% penicillin-streptomycin solution. The HT1080 human fibrosarcoma cells obtained from ATCC were grown in DMEM (high-glucose) supplemented with 10% FBS and 1% penicillin-streptomycin. Fixed numbers of cells were plated in 24-well plates in normal growth medium. Transient transfection was done 24 h later using Superfect reagent. Each transfection mix consisted of 1 μg of experimental plasmid along with 0.1 μg of pCMV-*Fluc* plasmid as the transfection control. Stable HT1080 cells expressing *pRluc8* were selected with 500 μg/mL geneticin, and for *pGFP^2-Rluc*, *pGFP^2-Rluc8*, and *pGFP^2-FRB-FKBP12-Rluc8* plasmids, 350 μg/mL zeocin. Cells with highest expression were judged by measuring RLUC activity using the substrate coelenterazine.

***In vitro* BRET^2 assay.** For BRET imaging and ratiometric calculations, the cells were seeded in equal number (typically 10,000 per well unless otherwise mentioned) in 48-well plates; 4 to 6 h later, the cells were washed with Dulbecco's PBS, with 50 μL of fresh Dulbecco's PBS then added. Just before CCD imaging, 50 μL of diluted Clz400 (0.75 μg/well final concentration in 48-well format) were added and the plates were placed inside the black box CCD imaging (either IVIS100 or IVIS200). All scans were done in luminescent mode using the sequential image acquisition feature, with 1-min integration times, a binning of 5, and a field-of-view set at 15 cm, unless otherwise mentioned. Photon outputs were measured using 500 to 570 nm and 370 to 450 nm band pass emission filters for GFP^2 and RLUC-Clz400 signal measurements, respectively. An hour later, FLUC signal was collected from individual wells by adding 0.1 μg of D-luciferin substrate per well. For single-cell imaging, the field of view was set to 4 cm by raising the platform. Images were analyzed using LIVING IMAGE v2.5 software (Caliper). For quantitation, regions of interests were drawn over the respective signals as visualized on the overlay image and mean average radiance (photons/s/cm^2/sr) was computed using the software tools.

Animal imaging of BRET^2 expression by using a cooled CCD camera. An aliquot of 0.5×10^6 HT1080 cells constitutively overexpressing either *pGFP^2-Rluc* or *pGFP^2-Rluc8* was injected s.c. in a set of four nude mice anesthetized with ketamine/xylazine (4:1). One hour after cell injection, Clz400 (25 μg/mouse) diluted in sterile Dulbecco's PBS (100 μL total volume) was injected via tail vein (i.v.) and the mice were then imaged immediately. Mice were scanned using first the GFP^2 and then the RLUC filter, with 2-min acquisitions each. For the deep tissue signal detection experiment, 2×10^6 *pGFP^2-Rluc8*–expressing cells were injected via tail vein in a set of five anesthetized nude mice and a scan was done half an hour later using a 75 μg/mouse injection of Clz400. The animals were placed supine in a light-tight chamber, and a gray-scale photographic reference image was obtained under low-level illumination. Photons emitted from implanted cells on mice were collected for 3 min using specified filter sets.

Statistical testing. Average radiance values were obtained from both cell culture assays and *in vivo* mouse experiments by drawing regions of interest on the images. These values were used for BRET^2 ratiometric calculations. All cell culture and mouse group comparisons were done with two-sided Student's *t* test using Microsoft EXCEL. $P < 0.05$ was considered statistically significant.

Results

Quantum-efficient mutant donors show significant improvement in the BRET efficiency. Generation and basic characterization of *Rluc* mutations were recently described by our lab (26). During the course of the study, we tested three of these mutant variants: (*a*) single-mutation C124A for increased stability (referred to as *Rluc-C*); (*b*) double-mutation C124A/M185V for both increased stability and high quantum yield (referred to as *Rluc-M*); and (*c*) combined eight-mutation *Rluc8* (incorporating A55T, C124A, S130A, K136R, A143M, M185V, M253L, and S287L point mutations) with markedly increased stability and even higher quantum yield than *Rluc-M*. These three mutant donors had been compared with the native *Rluc* for their luminous properties while using the native coelenterazine substrate and Clz400. As shown in Supplementary Table S1, after introduction of the mutations, marked increases in the activity (photon output) of the *Rluc-M* and *Rluc8* occur. The most characteristic changes are found while measuring the quantum yield of RLUC-M and RLUC8 with Clz400, indicating a key role of the M185V mutation for better utilization of the Clz400 substrate. Whereas RLUC-M and RLUC8 show only a 1.3-fold improvement in quantum yield compared with the native luciferase with coelenterazine, with Clz400, this increase in quantum yield is ~28- and ~32-fold, respectively. It was also noticed that in these mutants, the spectral properties are well maintained with a peak at ~482 ± 5 nm with coelenterazine and ~400 ± 5 nm with Clz400. In addition, for applications that require long-term monitoring of protein interactions, significant intracellular stability of RLUC8 should be advantageous for its use as a BRET donor.

To determine if donors with better quantum efficiencies could contribute in achieving better acceptor output, fusion plasmids were made by replacing native *Rluc* sequence with the mutated

donor sequences. The plasmids, including the linker (Ser-Gly-Ser-Ser-Leu-Thr-Gly-Thr-Arg-Ser-Asp-Ile-Gly-Pro-Ser-Arg-Ala-Thr), are otherwise identical to the *pGFP^2-Rluc* plasmid vector (22). The derived plasmid vectors incorporating *Rluc-C, Rluc-M*, and *Rluc8* mutation sequences are referred to as *pGFP^2-Rluc-C, pGFP^2-Rluc-M*, and *pGFP^2-Rluc8*, respectively. Both GFP fluorescence intensity and semiquantitative Western blot analysis show equivalent expression of the intact fusion protein in 293T cells transiently transfected with *pGFP^2-Rluc* and *pGFP^2-Rluc8* (Fig. 1*A* and *B*). However, in comparison with the cells expressing GFP^2-RLUC, the normalized donor and acceptor signals obtained by adding the Clz400 substrate show 35- and 80-fold higher signals for the GFP^2-RLUC8 fusion and 25- and 40-fold higher signals for GFP^2-RLUC-M, respectively. Following transfection of all the fusion plasmids along with the donor alone plasmids (e.g., *pRluc, pRluc-C, pRluc-M*, and *pRluc8*) in 293T cells, CCD imaging shows 3.4- and 5.5-fold

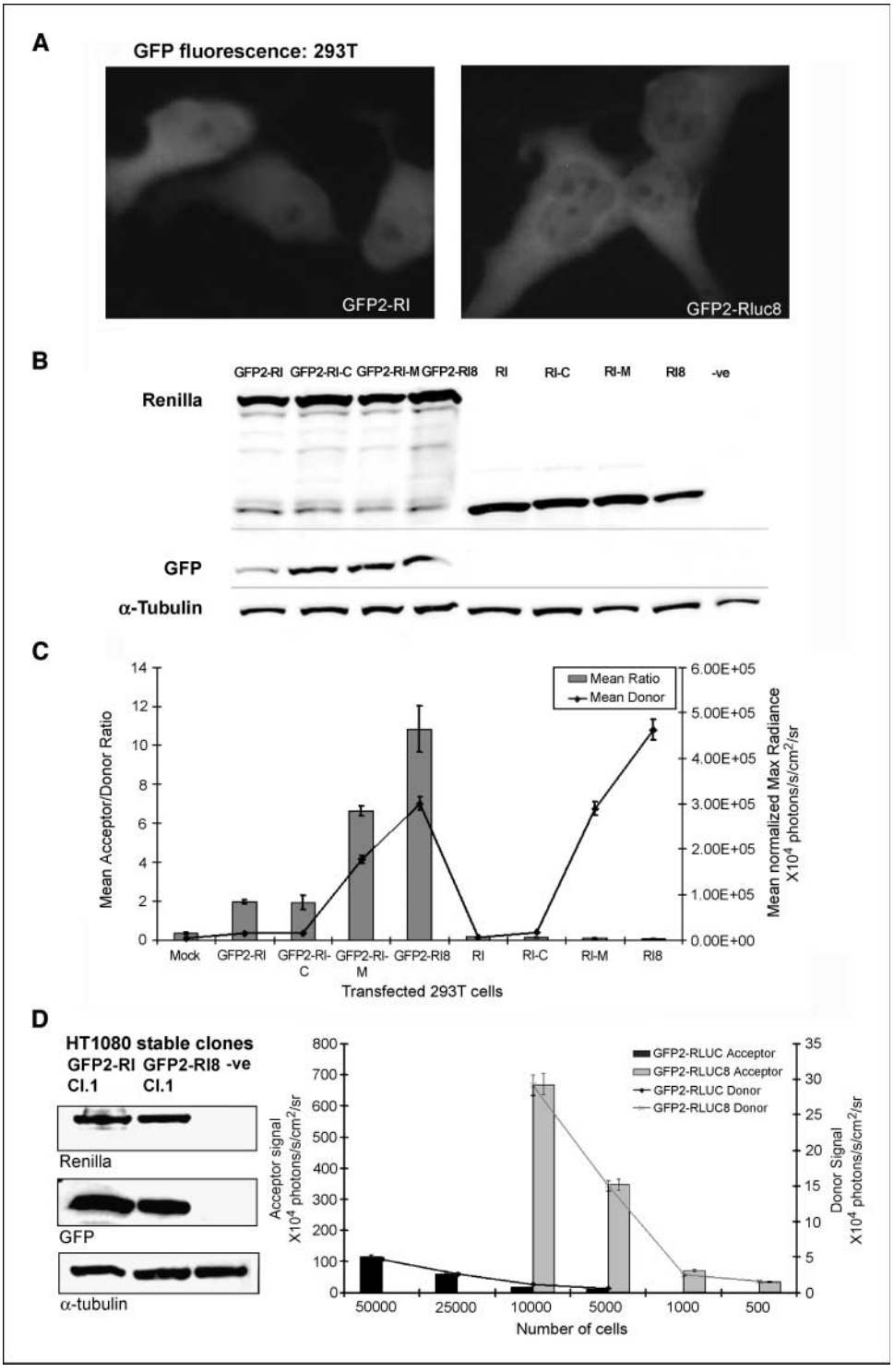

Figure 1. Mammalian expression of the new BRET vectors using *Renilla* luciferase mutants as donor. *A,* fluorescent photomicrographs of transiently transfected 293T cells expressing either GFP^2-RLUC or GFP^2-RLUC8 fusion 24 h after transfection. *B,* semiquantitative Western blot analysis showing donor (RLUC) and acceptor (GFP^2) protein expression in 293T cells transiently transfected with donor alone and fusion plasmids as marked. *GFP^2-Rluc-C, GFP^2-Rluc-M,* and *GFP^2-Rluc8* indicate BRET fusions using the single-mutation C124A RLUC, double-mutation C124A/M185V RLUC, and eight-mutation RLUC8 donors, respectively. α-Tubulin was used as loading control. *C,* the same cells as mentioned in (*B*) were plated (10,000 per well in a 48-well plate) and imaged with a CCD camera after adding equal amount of Clz400 substrate in each well. Mean photon values were determined by drawing regions of interest over triplicate samples. The chart represents the normalized mean BRET ratio (*columns*) and RLUC emission light outputs (*line*). *Bars,* SEM. *D,* semiquantitative assessment of BRET donor and acceptor proteins by Western blotting in selected clonal populations of HT1080 cells expressing the fusion constructs. α-Tubulin was used as a loading control. After checking the fusion protein expression in clonal populations, a fixed number of each cell type was plated and, within 4 h, CCD camera imaging was done by adding equal amount of Clz400 in well plates. Region of interest values from corresponding wells were plotted as obtained from image data using either a donor or acceptor filter. *Bars,* SEM.

increases in the BRET ratio following the characteristic gain in donor signals from RLUC-M and RLUC8 mutant donors (Fig. 1*C*). Light emission by proteins expressed from plasmids encoding only the donor is helpful in determining the bleed through photons with the GFP^2 filter, which was <5% for all constructs. Based on these results, it is clear that the *pGFP²-Rluc8* vector results in the highest gain in the dynamic range of the BRET signal, and this construct was therefore selected for further studies.

Mammalian cells constitutively overexpressing the GFP^2-RLUC8 fusion yield ~30-fold higher acceptor light signal than the GFP^2-RLUC fusion. HT1080 human fibrosarcoma cells constitutively overexpressing either GFP^2-RLUC or the GFP^2-RLUC8 fusion protein were established. Isolated clones were judged based on semiquantitative Western blotting results for equivalent expression of each fusion protein (Fig. 1*D*). After plating varying numbers of each cell type, CCD imaging was done following addition of equal amounts of Clz400 substrate. Figure 1*D* shows that the component light signals increase proportionately with cell number. By comparing the acceptor signals between the two cell lines, it was determined that every GFP^2-RLUC8 cell yields a signal equivalent to 30 GFP^2-RLUC–expressing cells. By comparing the donor signal, each GFP^2-RLUC8 cell yields signal equivalent to ~24 GFP^2-RLUC cells. By applying decay correction to the values of donor signal (see Supplementary data) to correct for signal decay due to the time lapse during scanning, we determined the BRET ratio as 8.6 ± 2.2 for individual cells (n = 5) expressing GFP^2-RLUC8.

Optical CCD camera imaging can spectrally resolve component light signals as a measure of the BRET signal from individual live cells constitutively overexpressing the GFP^2-RLUC8 fusion. To address the capability of BRET measurement from single cells, imaging was done with the established HT1080 cells constitutively overexpressing *pGFP²-Rluc*, *pRluc8*, or *pGFP²-Rluc8* within a few hours after plating. Previously, we reported that $BRET^2$ component signals can be resolved from ~30 cells transiently transfected with *pGFP²-Rluc* plasmid (22). Independent of cell types, this vector does not produce enough signal to allow individual cells stably overexpressing the GFP^2-RLUC fusion to be resolved, even with the aid of one of the most sensitive cooled CCD camera imaging system available (IVIS 200). Our results here with cells stably expressing RLUC8 as well as the GFP^2-RLUC8 fusion (Fig. 2*A*) show that when the total light output (open filter) is a combination of two major wavelengths of light, CCD imaging can spectrally resolve and quantify the component light signals from individual cells containing these new vectors. For individual cells expressing GFP^2-RLUC8, the average radiance with the GFP^2 filter is 2.5 ± 0.3 × 10^4 photons/s/cm^2/sr at 1 min and with the RLUC filter is 0.6 ± 0.1 × 10^4 photons/s/cm^2/sr at 3 min following

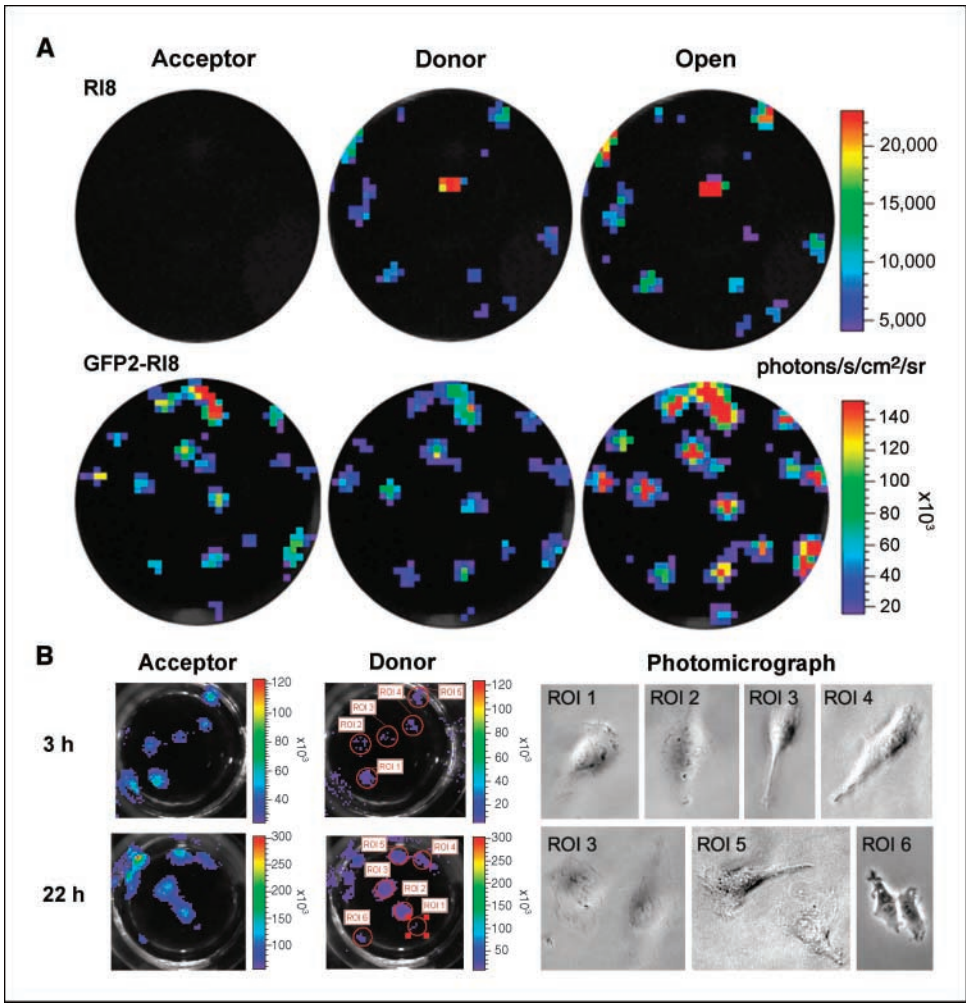

Figure 2. BRET signal can be spectrally resolved from mammalian cells expressing the BRET fusion vector. *A,* CCD camera image of a few HT1080 cells stably transfected with *Rluc8* and *GFP²-Rluc8* plasmid vector from individual wells of a 96-well plate. Cell imaging was done by adding Clz400 substrate (0.5 μg/well) 4 h after plating. Spectral separation of emission light from individual clonal cells transfected with native *Rluc* or *GFP²-Rluc* plasmid was not possible. Pseudocolor scale bar represents luminescence photon output averaged for the three filters. *B,* to confirm the true nature of signals from individual cells, parallel wells containing cells were imaged at 3 and 22 h after plating. As the cells divide over time, acceptor and donor signal intensities are doubled. Individual cells of the marked region of interest (*ROI*) locations were photographed with a light microscope after CCD imaging.

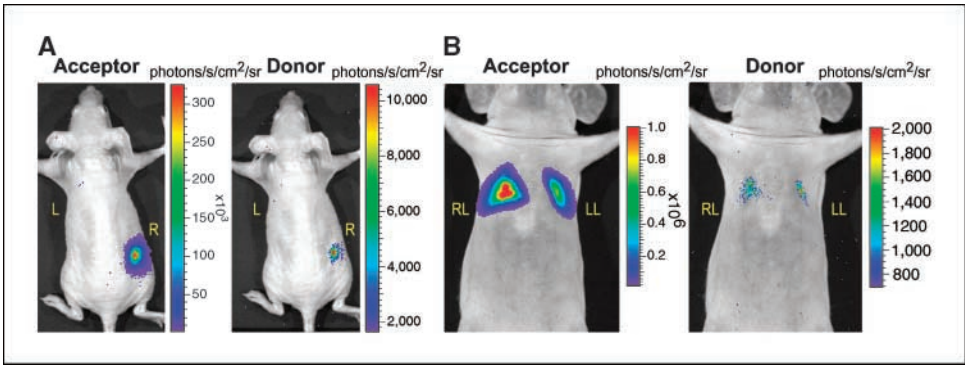

Figure 3. Localization of BRET signal from subcutaneous and deep tissue structures of a nude mouse implanted with cells constitutively overexpressing GFP^2-RLUC8. *A,* CCD camera image of a representative mouse implanted with 5×10^5 GFP^2-Rluc cells on the left shoulder (*L*) and the same number of GFP^2-Rluc8 cells on the right flank (*R*). The mice were injected with 25-μg Clz400 substrate via tail vein and imaged using a 2-min image acquisition time. *B,* CCD camera image of a representative mouse injected with 2×10^6 GFP^2-Rluc8 cells by tail-vein injection. Thirty minutes later, the mouse was injected with 75-μg Clz400 and imaged immediately using a 3-min acquisition time. Unlike cells that stably express GFP^2-RLUC, both donor and acceptor signals from GFP^2-Rluc8 expression can be measured from the lungs. For both (*A*) and (*B*), images were first captured using the GFP filter followed by the DBC filter after a single injection of Clz400.

addition of Clz400. The photon value obtained with an open filter image of the same cells captured at 5 min is nearly the same as the sum of the two component signals.

Further evaluation of single cells was done by allowing cells to grow in culture and then imaging at different time points with equal amounts of Clz400 substrate (Fig. 2*B*). As shown in the figure, selected region of interest locations were further documented by observing these locations using a light microscope. The average photon value for well-isolated individual cells at the 3-h time point is $2.8 \pm 0.3 \times 10^4$ and $0.5 \pm 0.1 \times 10^4$ photons/s/cm^2/sr with acceptor and donor filters, respectively, which doubled ($7.1 \pm 0.5 \times 10^4$ and $1.3 \pm 0.9 \times 10^4$ photons/s/cm^2/sr, respectively) as the cells divide at 22 h. Because these values are well above background ($0.4 \pm 0.03 \times 10^4$ photons/s/cm^2/sr; $P < 0.05$), we reasoned that this approach can be extended to studies monitoring BRET signal from specific protein-protein interactions in live individual cells.

The RLUC8 mutant donor signal can be noninvasively monitored in real time from superficial as well as deeper tissues in living mice. A comparison was done by implanting 5×10^5 HT1080 cells overexpressing either *pGFP^2-Rluc* or *pGFP^2-Rluc8* plasmids in the same mouse. The average radiance from *pGFP^2-Rluc8*–expressing cells yields $49 \pm 8 \times 10^3$ and $1.7 \pm 0.2 \times 10^3$ photons/s/cm^2/sr with the acceptor and donor filters, respectively. This is significantly ($P < 0.05$) higher than the values of $0.6 \pm 0.2 \times 10^3$ and $0.9 \pm 0.1 \times 10^3$ photons/s/cm^2/sr, respectively, obtained from *pGFP^2-Rluc* cells (Fig. 3*A*). The photon values obtained from stable HT1080 cells expressing GFP^2-RLUC are close to the background value ($0.3 \pm 0.5 \times 10^3$) and, therefore, the minimum detectable numbers of these cells should be $>5 \times 10^5$. Further, both GFP and RLUC component light signals from greater tissue depths were shown to be detectable from lungs by injecting a minimum of 2×10^6 HT1080 cells overexpressing GFP^2-RLUC8 via tail vein followed by an increased amount of Clz400 substrate injection (Fig. 3*B*). The average radiance of GFP signal from cells that are trapped in the lungs is $22.4 \pm 0.8 \times 10^4$ photons/s/cm^2/sr, in comparison with a background value from the lower abdomen of $0.38 \pm 0.03 \times 10^3$ photons/s/cm^2/sr. By turning the filter wheel, the RLUC8 signals collected in the subsequent minutes yield an average radiance of $0.37 \pm 0.1 \times 10^3$ and $0.42 \pm 0.06 \times 10^2$ photons/s/cm^2/sr for the donor and open filters, respectively. These results indicate that BRET-specific acceptor signal can be detected from even a lower number of cells, but due to increased tissue attenuation of shorter wavelength light, the donor signal quantitation needed to obtain a true BRET ratio measurement may be limited in small living subjects at greater depths.

A GFP^2-RLUC8 BRET sensor with FKBP12 and FRB as interacting partners can detect rapamycin-mediated heterodimerization *in vivo* at picomolar drug concentrations. To show the advantage of the new BRET vector, we designed a single vector sensor construct to measure rapamycin-mediated dimerization of the two mTOR pathway proteins, FKBP12 and FRB. Previously, we have observed that the FRB domain fused to the COOH terminus of GFP^2 and FKBP12 fused to the NH_2 terminus of RLUC successfully show BRET signal as a result of FKBP12 and FRB interaction in the presence of rapamycin (22). Based on that observation, a fusion construct was made by placing FRB and FKBP12 sequences in the linker region of the *pGFP^2-Rluc8* plasmid as shown in Fig. 4A. HT1080 cells stably overexpressing the vector were used for an imaging-based BRET assay. At first, the rapamycin dose-response results (Fig. 4*B*) show that a significant ($P < 0.05$) increase in the BRET signal can be obtained between 1 and 80 nmol/L of rapamycin, with a peak ratio of 6.8 at 40 nmol/L. Next, the BRET ratio was determined by exposing cells to 20 nmol/L rapamycin at various time points (Fig. 4*C*). Starting from a basal BRET ratio of 1.7 for cells incubated without rapamycin, the ratio increased significantly ($P < 0.05$) to a value of 6.1 at 8 h. A few cells were plated and once these cells settled in isolation, they were exposed to 40 nmol/L rapamycin and imaged over time, showing that although the growing number of cells at multiple locations shows donor and acceptor signal increments, the BRET ratio remains constant independent of cell number (Fig. 4*D*). By exposing or withdrawing rapamycin from the culture medium, we attempted visualization of the reversible nature of the BRET signal (Fig. 5*A*). On exposure of cells to 40 nmol/L rapamycin for 4 h, a BRET ratio of 4.4 is observed. As rapamycin is withdrawn and cells are maintained in a rapamycin-free environment, the signal drops significantly over 120 h, with the BRET ratio dropping to 2.65. When the cells are reexposed to 40 nmol/L rapamycin, a BRET value of 5.7 is observed, which is significantly above ($P < 0.05$) the value of 1.8 for cells never exposed to rapamycin.

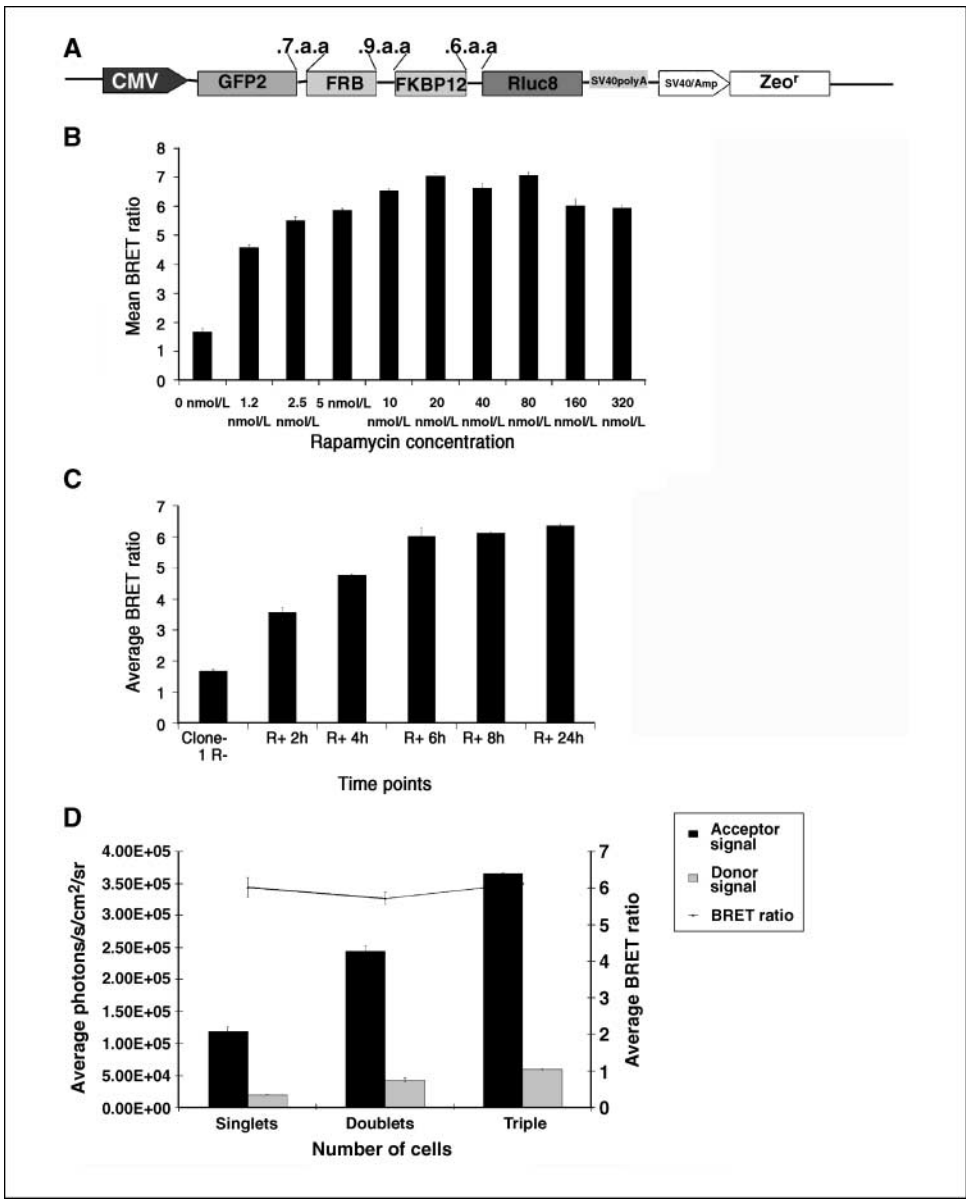

Figure 4. Characterization of a BRET sensor for testing a small-molecule dimerizer drug in mammalian cells. *A,* diagram showing the BRET vector construct, where two individual mTOR pathway protein sequences (FRB and FKBP12) were cloned between the donor and acceptor molecules using the specified amino acid linkers. FKBP12 and FRB domains dimerize only in the presence of the small-molecule dimerizer rapamycin, bringing the acceptor and donor in close proximity. *B,* HT1080 cells constitutively overexpressing the sensor vector were exposed to measured quantities of rapamycin for 20 h and then the BRET signal was quantitated by imaging with the Clz400 substrate. *C,* the same cells were exposed to 40 nmol/L rapamycin and the BRET signal was measured at various time points after addition of drug. *D,* a few cells were plated in a 96-well black plate and the BRET signal (*line*) was determined from individual cells or cells dividing over time, showing that although the acceptor and donor signals (*columns*) increase, the BRET ratio remains constant (at a specific drug concentration).

Rapamycin-mediated dimerization of stably overexpressing heteromeric proteins can be measured from single cells. To evaluate the utility of the current BRET sensor for rapid screening of drugs from a minimal number of cancer cells, we attempted assessment of protein functions by measuring the BRET signal from individual cells (Fig. 5*B*). Stably selected HT1080 cells overexpressing the GFP^2-FRB-FKBP12-RLUC8 fusion protein were plated in isolation and exposed to different concentrations of rapamycin. The cells maintained in culture without rapamycin do not have interaction of the FRB and FKBP12 domains; therefore, the acceptor and donor moieties are farther apart, resulting in only background signal. With increasing rapamycin concentrations, greater numbers of FRB and FKBP12 domains interact, which results in a conformational change of the fusion protein, bringing the acceptor and donor moieties in closer proximity. This leads to a significant increase of the acceptor signal to levels above background. We predict that this strategy should be useful for rapid screening of chemical compounds that function as modulators in various cellular protein networks.

Discussion

The use of BRET has the potential to significantly increase our understanding of cellular protein networks, especially as this method is further improved (27). In addition to taking advantage of advanced cooled-CCD detector based systems (22, 28), further improvements in BRET technologies are currently under active investigations to achieve higher sensitivity and suitability for measurements in physiologically relevant model systems. In this study, for the first time, a BRET system is described that can assess protein interactions with high sensitivity from both live individual cells and small living animals. In brief, we have tested donor contributions to the well-known GFP^2-RLUC (BRET^2) systems by altering the native *Renilla* luciferase sequence with mutations known to increase stability and quantum yield. The eight mutations leading to RLUC8 have greatly improved the donor contribution to the acceptor moiety, thereby increasing the overall sensitivity of the system. This new BRET fusion should be useful for increasing the overall sensitivity of the BRET system,

irrespective of the measurement instrument used, leading to either shorter acquisition times and/or allowing use of lower substrate concentration and thus minimizing errors in ratiometric calculations and dependence on decay correction factors of the donor light.

Conceptually, the Förster distance, R_0 (29), is calculated based on the following equation:

$$R_0 = 2.11 \times 10^{-2} \cdot [\kappa^2 \cdot J(\lambda) \cdot \eta^{-4} \cdot Q_D]^{1/6}$$

where κ^2 is the relative orientation between the transition dipoles of the donor and acceptor, $J(\lambda)$ is the overlap integral in the region of the donor emission and acceptor absorbance spectra (with the wavelength expressed in nanometers), η represents the refractive index of the medium, and Q_D is the donor quantum yield. Summarizing the basic concepts of resonance energy transfer, one can critically relate the rate of energy transfer with the important variables [κ^2, $J(\lambda)$, η, and Q_D], of which the Q_D dependence is taken advantage of in the current work. Because of the sixth-root dependence in the calculation of R_0, small errors or uncertainties in the value of Q_D do not have a large effect on the overall BRET efficiency. Our results clearly indicate that, as a result of using a variant of the donor protein with a 35-fold gain in donor quantum yield, marked improvement in the overall efficiency of the BRET system results, at least when the acceptor moiety is a variant of *Aequorea* GFP. Clz400 has previously been known to result in extraordinary low light output when used with native RLUC (30), which stems mainly from poor quantum yield with this substrate (see Supplementary Table S1). Previous work in our laboratory using a strategy of consensus sequence–based semi-rational mutagenesis of *Renilla* luciferase resulted in identification of mutations that greatly increased the quantum yield of *Renilla* luciferase (26), especially when used with Clz400. During this study, we picked these previously identified variants of *Renilla* luciferase as BRET donors to verify the Q_D dependence of the BRET signal, while obtaining a photon-efficient BRET vector. Among the vectors generated, as the RLUC8 protein is ~1 order of magnitude more stable than RLUC in the cytoplasmic environment, use of the double-mutation RLUC (C124A/M185V) as a BRET pair with GFP^2 could be useful for applications where stability of the donor protein is not preferred. The BRET vector using RLUC8, which exhibits increased stability and a 60-fold improvement in light output

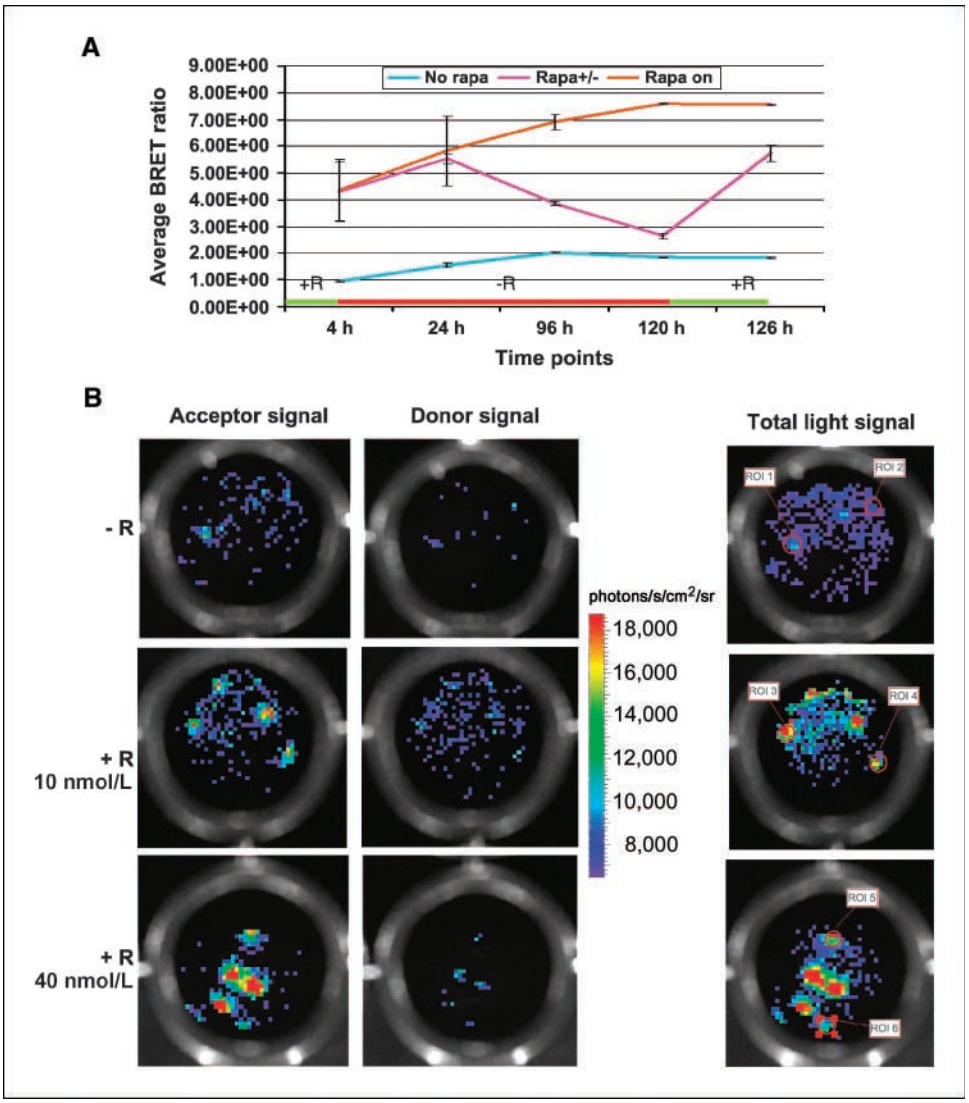

Figure 5. CCD camera images of individual HT1080 cells constitutively overexpressing the GFP^2-FRB-FKBP12-Rluc8 fusion in the presence or absence of rapamycin. *A,* HT1080 cells expressing the GFP^2-FRB-FKBP12-RLUC8 fusion were also used to determine the reversible nature of the BRET signal. Positive control (*dark dotted line*) cells were constantly incubated in medium containing 40 nmol/L rapamycin and negative control (*light dotted line*) cells were incubated in normal medium. The experimental cells (*solid line*) were first incubated in rapamycin (40 nmol/L)–containing medium for 4 h, imaged, and then maintained in rapamycin-free medium until the signal dropped significantly (120-h scan time point). After imaging at this time point, the cells were reexposed to rapamycin (40 nmol/L) for 5 h and imaged again showing increased BRET signal. *B,* a 96-well plate containing a few stably selected HT1080 cells expressing the GFP^2-FRB-FKBP12-RLUC8 fusion were subjected to different doses of rapamycin as marked and imaged using a CCD camera 4 h after plating. Individual cells were below detectable threshold with the substrate concentration (0.5 μg/well) and the CCD integration time (1 min) used. With increasing drug concentration, as the interacting partners dimerize, the BRET partners come in closer proximity, leading to a higher BRET signal and thus enabling detection of BRET-specific GFP signal from individual cells. Pseudocolor scale bar represents the average luminescence photon output.

with the Clz400 substrate, results in the highest improvement in the BRET signal. Previously, we attempted BRET signal detection from mouse models (22) using a *GFP²-Rluc* vector and observed that both the minimum numbers of detectable cells and the required image acquisition time were relatively high. The current BRET vector has shown significant improvements to overcome each of these limitations, with significantly lower number of cells constitutively overexpressing the BRET partners needed for detectability and/or reduced scan times. Furthermore, improvements were also observed for imaging the BRET signal from deep tissue structures, where both robust acceptor signal and attenuated emission donor signal were captured from the lungs.

Transfection of mammalian cells with the GFP² fusion plasmids using *Rluc-M* and *Rluc8* as the donors, in comparison with the native *Rluc*-containing fusion plasmid, confirms that significantly higher (25- and 35-fold, respectively) donor light output is translated into higher acceptor light output. Interestingly, the fold gain in observed acceptor light output from the *GFP²-Rluc-M* and *GFP²-Rluc8* constructs is even higher (40- and 80-fold, respectively), resulting in 3.3- and 5.5-fold increases in the BRET ratio, respectively. Further, by comparing the light signals from stable HT1080 cells with equivalent expression of the donor and acceptor proteins, each cell that expresses GFP²-RLUC8 shows ~24-fold higher donor signal and 30-fold higher acceptor signal in comparison with GFP²-RLUC–expressing cells. Considering results from stable cells as less error-prone, these results clearly indicate that the increased donor quantum yield does make a significant difference in BRET acceptor signal.

By using the *GFP²-Rluc*8 vector, we attempted live cell imaging of single cells directly from culture dishes by diluting the HT1080 stable cells to very low densities. The results indicate that both donor and acceptor signals from individual cells are much higher than the background signal and thus can be spectrally resolved. Previously, single-cell imaging of bioluminescent light has been attempted using microscopes with an attached CCD (31, 32), where the resultant luminescence signal comes from a direct donor-acceptor fusion or by transcriptional control of a circadian rhythm gene. With the new BRET vector described in the current work, we were able to show for the first time that BRET signal as a function of protein conformational changes can also be monitored from single cells using a cooled CCD. As a demonstration model, we choose two mTOR pathway proteins where the mTOR-targeting molecule rapamycin was shown to work as a gain-of-function mechanism in which it binds to the intracellular protein FKBP12. The FKBP12-rapamycin complex is known to form heterodimers with a FRAP binding domain called FRB, an event which is documented here from single intact cells. Evaluation of drug response from single cells can help to study heterogeneous cell behavior in cell culture and lead to improved sensitivity for *in vivo* applications, allowing the study of much fewer cells in living animal models. For most cases, by quantitating the signal intensities, it is possible to differentiate the numbers of cells residing at each location. However, as the minimum field of view of the camera is 4 cm in diameter, subcellular resolution is hard to achieve with the current imaging instrument.

The new BRET vector developed in the current work should be ideal for use as a sensitive assay *in vitro*, for single live cells *in vivo*, and from living population of cells within small living subjects. The added sensitivity to the known BRET system should also empower drug screening from 384-well plates with few live cells per well, constitutively overexpressing genetic sensors, enabling an automated imaging strategy for high-throughput application of BRET technology.

Acknowledgments

Received 12/18/2006; revised 5/17/2007; accepted 5/24/2007.

Grant support: NIH grant 5RO1 CA82214 (S.S. Gambhir) and National Cancer Institute *In vivo* Cellular and Molecular Imaging Center grant P50 CA114747 (S.S. Gambhir), Center for Cancer Nanotechnology Excellence grant U54 CA119367 (S.S. Gambhir), and National Cancer Institute Small Animal Imaging Resource Program.

The costs of publication of this article were defrayed in part by the payment of page charges. This article must therefore be hereby marked *advertisement* in accordance with 18 U.S.C. Section 1734 solely to indicate this fact.

References

1. Hidalgo M, Rowinsky EK. The rapamycin-sensitive signal transduction pathway as a target for cancer therapy. Oncogene 2000;19:6680–6.
2. Guertin DA, Sabatini DM. An expanding role for mTOR in cancer. Trends Mol Med 2005;11:353–61.
3. Sarbassov DD, Ali SM, Sengupta S, et al. Prolonged rapamycin treatment inhibits mTORC2 assembly and Akt/PKB. Mol Cell 2006;22:159–68.
4. Arnold LA, Estebanez-Perpina E, Togashi M, et al. A high-throughput screening method to identify small molecule inhibitors of thyroid hormone receptor coactivator binding. Sci STKE 2006;2006:pl3.
5. Ravichandran V, Sabath BF, Jensen PN, Houff SA, Major EO. Interactions between c-Jun, nuclear factor 1, and JC virus promoter sequences: implications for viral tropism. J Virol 2006;80:10506–13.
6. Seitz H, Hutschenreiter S, Hultschig C, et al. Differential binding studies applying functional protein microarrays and surface plasmon resonance. Proteomics 2006; 6:5132–9.
7. Eidne KA, Kroeger KM, Hanyaloglu AC. Applications of novel resonance energy transfer techniques to study dynamic hormone receptor interactions in living cells. Trends Endocrinol Metab 2002;13:415–21.
8. Keppler A, Gendreizig S, Gronemeyer T, et al. A general method for the covalent labeling of fusion proteins with small molecules *in vivo*. Nat Biotechnol 2003;21:86–9.
9. Germain-Desprez D, Bazinet M, Bouvier M, Aubry, M. Oligomerization of transcriptional intermediary factor 1 regulators and interaction with ZNF74 nuclear matrix protein revealed by bioluminescence resonance energy transfer in living cells. J Biol Chem 2003;278:22367–73.
10. Schaaf CP, Benzing J, Schmitt T, et al. Novel interaction partners of the TPR/MET tyrosine kinase. FASEB J 2005;19:267–9.
11. Perroy J, Pontier S, Charest PG, Aubry M, Bouvier M. Real-time monitoring of ubiquitination in living cells by BRET. Nat Methods 2004;1:203–8.
12. Xu X, Meier-Schellersheim M, Jiao X, Nelson LE, Jin T. Quantitative imaging of single live cells reveals spatiotemporal dynamics of multistep signaling events of chemoattractant gradient sensing in *Dictyostelium*. Mol Biol Cell 2005;16:676–88.
13. Massoud TF, Gambhir SS. Molecular imaging in living subjects: seeing fundamental biological processes in a new light. Genes Dev 2003;17:545–80.
14. Wu JC, Inubushi M, Sundaresan G, Schelbert HR, Gambhir SS. Optical imaging of cardiac reporter gene expression in living rats. Circulation 2002;105:1631–4.
15. Ray P, Pimenta H, Paulmurugan R, et al. Noninvasive quantitative imaging of protein-protein interactions in living subjects. Proc Natl Acad Sci U S A 2002;99:3105–10.
16. Luker GD, Sharma V, Pica CM, et al. Noninvasive imaging of protein-protein interactions in living animals. Proc Natl Acad Sci U S A 2002;99:6961–6.
17. Luker KE, Piwnica-Worms D. Optimizing luciferase protein fragment complementation for bioluminescent imaging of protein-protein interactions in live cells and animals. Methods Enzymol 2004;385:349–60.
18. Ozawa T, Kaihara A, Sato M, Tachihara K, Umezawa Y. Split luciferase as an optical probe for detecting protein-protein interactions in mammalian cells based on protein splicing. Anal Chem 2001;73:2516–21.
19. Paulmurugan R, Gambhir SS. Monitoring protein-protein interactions using split synthetic renilla luciferase protein-fragment-assisted complementation. Anal Chem 2003;75:1584–9.
20. Paulmurugan R, Gambhir SS. An intramolecular folding sensor for imaging estrogen receptor-ligand interactions. Proc Natl Acad Sci U S A 2006;103: 15883–8.
21. Paulmurugan R, Massoud TF, Huang J, Gambhir SS. Molecular imaging of drug-modulated protein-protein interactions in living subjects. Cancer Res 2004;64: 2113–9.
22. De A, Gambhir SS. Noninvasive imaging of protein-protein interactions from live cells and living subjects using bioluminescence resonance energy transfer. FASEB J 2005;19:2017–9.
23. So MK, Xu C, Loening AM, Gambhir SS, Rao J.

Self-illuminating quantum dot conjugates for *in vivo* imaging. Nat Biotechnol 2006;24:339–43.
24. Xu Y, Piston DW, Johnson CH. A bioluminescence resonance energy transfer (BRET) system: application to interacting circadian clock proteins. Proc Natl Acad Sci U S A 1999;96:151–6.
25. Dionne P, Mireille C, Labonte A, et al. BRET2: efficient energy transfer from Renilla luciferase to GFP2 to measure protein-protein interactions and intracellular signaling events in live cells. In: van Dyke K, van Dyke C, Woodfork K, editors. Luminescence biotechnology: instruments and applications. Boca Raton (FL): CRC Press; 2002. p. 539–55.
26. Loening AM, Fenn TD, Wu AM, Gambhir SS. Consensus guided mutagenesis of Renilla luciferase yields enhanced stability and light output. Protein Eng Des Sel 2006;19:391–400.
27. Pfleger KD, Eidne KA. Illuminating insights into protein-protein interactions using bioluminescence resonance energy transfer (BRET). Nat Methods 2006;3:165–74.
28. Ayoub MA, Couturier C, Lucas-Meunier E, et al. Monitoring of ligand-independent dimerization and ligand-induced conformational changes of melatonin receptors in living cells by bioluminescence resonance energy transfer. J Biol Chem 2002;277:21522–8.
29. Forster T. Zwischenmolekulare energiewanderung und fluoreszenz. Ann Phys 1948;2:54–75.
30. Hart RC, Matthews JC, Hori K, Cormier MJ. *Renilla reniformis* bioluminescence: luciferase-catalyzed production of nonradiating excited states from luciferin analogues and elucidation of the excited state species involved in energy transfer to Renilla green fluorescent protein. Biochemistry 1979;18:2204–10.
31. Welsh DK, Kay SA. Bioluminescence imaging in living organisms. Curr Opin Biotechnol 2005;16:73–8.
32. Welsh DK, Yoo SH, Liu AC, Takahashi JS, Kay SA. Bioluminescence imaging of individual fibroblasts reveals persistent, independently phased circadian rhythms of clock gene expression. Curr Biol 2004;14:2289–95.

An Improved Bioluminescence Resonance Energy Transfer Strategy for Imaging Intracellular Events in Single Cells and Living Subjects

Abhijit De, Andreas Markus Loening and Sanjiv Sam Gambhir

Cancer Res 2007;67:7175-7183.